Optimal Control Aided by the ELECTRE III Multicriteria Decision Method Applied to Quadcopter Autopilot

Lucas de Carvalho Sodré * **Antonio da Silva Silveira** *
Marcos César da Rocha Seruffo *

* *Laboratory of Control and Systems, Federal University of Pará, PA (e-mail: lucas.sodre@itec.ufpa.br, asilveira@ufpa.br, seruffo@ufpa.br).*

Abstract: Unmanned aerial vehicles, such as quadcopters, can perform several activities. To enable such activities, it is necessary to use control techniques to guarantee the completion of the task amid environmental adversities. In this work, multivariable control was used, known as Linear Quadratic Regulator, which features optimal control based on weighting matrices, which were tuned based on the Elimination and Choice Expressing Reality III multicriteria decision method, where the criteria are the desired performance and robustness characteristics for the task the drone was assigned to. This application is used as a basis for an estimated model based on experimental flights of Parrot's AR. Drone 2.0 quadcopter, thus introducing actual flight conditions into the proposed control project. The simulated results show that the controller tuning, selected with the aid of the Elimination and Choice Expressing Reality III method, obtained performance indices (Integral Squared Error and Integral Quadratic Control effort indices) and robustness (gain margin and phase margin) consistent with the objectives of the control project, thus establishing itself as a practical alternative in helping the designer in choosing controller parameters.

Keywords: Quadcopter, Multicriteria Decision Method, Multiple Inputs Multiple Outputs.

1. INTRODUCTION

Recently, aerospace systems called Unmanned Aerial Vehicles (UAVs) have attracted increasing interest from researchers due to the challenging dynamics, uncertainties, disturbances, and rapid change to which they are subject (Elkhatem and Engin, 2022). There are several examples of applications such as military and civil surveillance, logistics, forest fire monitoring (David W. Casbeer and McLain, 2006), data collection, data acquisition, wireless powered communication network (Wang et al., 2021) and so on. The quadcopter vehicle is one of the most suitable for carrying out these tasks due to its peculiar characteristics such as small size, ease of take-off and landing in a small space, and less mechanical and hardware complexity when compared to other UAVs.

However, quadcopters, popularly called 'drones,' are more susceptible to various disturbances and uncertainties during flight, making their control systems' robustness, reliability, and acceptable performance important. Different control strategies were proposed to control the dynamics of the UAV, some were based on linear control theories, such as the proportional integral derivative (PID) controller (Khatoon et al., 2014), Linear Quadratic Regulator (LQR) (Reyes-Valeria et al., 2013), and H-infinity (López et al., 2015).

LQR control techniques have been extensively investigated to control drone dynamics, as it is an optimal control methodology based on minimizing a given cost function (Tahir et al., 2016). The quadratic cost function of the LQR controller has two variables called weighting matrices, matrices Q and R, where the matrix Q weights the errors in the trajectories of the state variables. In contrast, the weighting matrix R is associated with control effort and actuator saturation. Therefore, the LQR controller offers the designer an optimal solution according to the preferences expressed in the Q and R matrices. Therefore, the process of choosing matrix values must be based on the project requirements, and often, their values must be adjusted using a trial-and-error method.

Evolution-based optimization algorithms have been developed recently to obtain a more systematic method for fitting Q and R matrices. In Joelianto et al. (2020), the work focused on designing a tracking control for the drone swarm based on LQR combined with a genetic algorithm, which optimally selects the weighting matrices Q and R. In the work of Kumar and Jerome (2016), is proposed an analytical relationship between the Riccati algebraic equation and the Lagrangian optimization principle as an alternative method to solve the LQR weight selection problem in the tracking control of a magnetic levitation system—third order. Finally, in the article by Xiong and Zhang (2016), the selection method for LQR weighting matrices was developed based on a reformulation of the conventional LQR design problem as an optimization problem. An adaptive optimization algorithm, particle swarm, was used. Applying these different evolution algorithms could obtain different solutions for the same control crite-

ria. Therefore, the literature has no perfect and commonly accepted method for adjusting weighting matrices.

It can be assumed that the works cited aim to select the best weights for the weighting matrices based on optimization (algorithms that aim for the best solutions) of optimization (LQR algorithm that guarantees the optimal tuning of the regulator). In this work, the proposed approach adapts the optimization, thus finding the tuning that best suits the control projects among the optimal solutions from the LQR algorithms. Therefore, the focus is not only on the closed circuit's performance and robustness criteria but also on comparing different adjustment alternatives to select the solution that best meets the design criteria. Therefore, this article applied the Multi-Criteria Decision Making Model (MCDM) Elimination and Choice Expressing Reality (ELECTRE) III to find the best values of the weighting matrices of an LQR control project. This LQR, with ELECTRE III assisted tuning, is designed to control the autopilot system of Parrot's AR.Drone 2.0 quadcopter.

Such models that assist decision-making have been widely used to tune controllers. In the work Wang et al. (2017), Data Envelopment Analysis was used to evaluate and diagnose the performance of the PID control circuit depending exclusively on process data collected during routine plant operation. In the article by Srikanth and Yadaiah (2020), the Preference Ranking Organization Method for Enrichment Evaluations technique readjusts the first-order process control system with delay, obtaining a more verisimilitude model for the plant's dynamics. Finally, work by Srikanth and Yadaiah (2021) the Analytical Hierarchical Process algorithm tunes control parameters to mitigate active system disruption.

This work aims to adapt the values of the weighting matrices to the control project. For this, the ELECTRE III model was used to rank the weighting matrix configurations that are most aligned with the task criteria in which it will be required, choosing the tuning of the LQR algorithm. The LQR was designed for the quadcopter's autopilot system, which is used as a basis for the linear model raised by data obtained from experimental flights of Parrot's Ar.Drone 2, imposing real scenarios in simulated tests of the algorithm. Several tuning alternatives are designed based on the model, and the ELECTRE III method is responsible for ranking the best LQR tuning for the required task.

2. METHODOLOGY

This Section will present the LQR's fundamentals, the ELECTRE III and its design criteria, the quadcopter model, and the LQR tuning.

2.1 Linear Quadratic Regulator

LQR is an optimal regulator that can be designed for both MIMO and SISO (Ogata, 1996) systems. LQR aims to find a set of gains that allows an optimized trajectory of the system states to its equilibrium point. In the Equation (1) is the discrete model in state space, to which the LQR is subject:

$$\begin{aligned} \mathbf{x}(k) &= \mathbf{A}\mathbf{x}(k-1) + \mathbf{B}\mathbf{u}(k-1) \\ \mathbf{y}(k) &= \mathbf{C}\mathbf{x}(k) \end{aligned} \tag{1}$$

Based on the linear system, the LQR algorithm minimizes the cost function in Equation (2), where $\mathbf{J}$ is the cost function, $\mathbf{Q}$ is a (semi-) definite positive, and $\mathbf{R}$ is a definite positive. These matrices determine the optimal controller tuning.

$$\mathbf{J} = \sum_{k=0}^{\infty} \left(\mathbf{x}_k^T \mathbf{Q} \mathbf{x}_k + \mathbf{u}_k^T \mathbf{R} \mathbf{u}_k \right) \tag{2}$$

Using the cost function, we look for the value of $\mathbf{K}_c$ that optimizes the trajectory of the states as described in the Equation (3).

$$\mathbf{u}(k) = \mathbf{K}_c \, \mathbf{x}(k) \tag{3}$$

where $\mathbf{K}_c$ is calculated based on the minimization of the covariance matrix of the states found iteratively in discrete time by the dynamic Riccati equation as described in Ogata (1996).

In this way, the LQR algorithm calculates gains that optimize the trajectory of states toward the system's equilibrium point. These values change based on the coefficients of the matrices $\mathbf{Q}$ and $\mathbf{R}$. Selecting significant coefficients for the $\mathbf{R}$ matrix means that the designer applies a larger penalty to the control effort to optimize the cost function, also known as a low-cost control solution; in contrast, selecting small coefficients means trying to stabilize the system with an expensive control strategy. Likewise, if the designer chooses large coefficients for the $\mathbf{Q}$ matrix, this means trying to stabilize the system with as few state changes as possible. In contrast, a $\mathbf{Q}$ matrix with small coefficients implies less concern about state changes.

The control objective in this work is the application of LQR to reference tracking of the frontal displacement, lateral displacement, and height of the quadcopter. To guarantee zero stationary error in the reference track, the controller must be designed for the extended model of the system, controlling the states and their variations, as discussed in work by Silveira et al. (2020). This extended model of the system is represented in the Equation (4), with the state feedback control law based on the Equation (6) where $\mathbf{r}(k)$ is the reference vector of the states.

$$\overbrace{\begin{bmatrix} \mathbf{y}(k) \\ \Delta\mathbf{x}(k) \end{bmatrix}}^{\mathbf{x}_a(k)} = \overbrace{\begin{bmatrix} \mathbf{I} & \mathbf{CA} \\ \mathbf{0} & \mathbf{A} \end{bmatrix}}^{\mathbf{A}_a} \begin{bmatrix} \mathbf{y}(k-1) \\ \Delta\mathbf{x}(k-1) \end{bmatrix} + \overbrace{\begin{bmatrix} \mathbf{CB} \\ \mathbf{B} \end{bmatrix}}^{\mathbf{B}_a} \Delta\mathbf{u}(k-1) \tag{4}$$

$$\mathbf{y}(k) = \overbrace{[\mathbf{C} \ \mathbf{0}]}^{\mathbf{C}_a} \mathbf{x}_a(k) \tag{5}$$

$$\Delta\mathbf{u}(k) = \mathbf{K} \left(\mathbf{r}(k) - \mathbf{x}_a(k) \right) \tag{6}$$

The discrete difference operator is represented by $\Delta = 1 - q^{-1}$, where q^{-1} is the discrete-time backward shift operator, $\Delta\mathbf{u}(k)$ is the control increment, $\mathbf{C}$ is the matrix

that correlates the states with the outputs controlled by the LQR and $\mathbf{C}_a$ is its extended version. Therefore, the control law described in the Equation (7) is the control signal to be applied to the system input, which can be easily implemented in a digital computer to obtain incremental control.

$$\mathbf{u}(k) = \mathbf{u}(k-1) + \Delta\mathbf{u}(k) \tag{7}$$

Based on the augmented system, there are increased weighting matrices, $\mathbf{Q}_a$ and $\mathbf{R}_a$, making it necessary to propose values for the new states created. The method of choosing such values will be discussed later in the work.

2.2 System Model

The discrete state space model used to tune the LQR and create the simulated environment was raised in Sodré (2024) describing not only the dynamics of the drone but also the disturbances that affect the system, thus a stochastic model of the AR.Drone 2.0. This model has the states of altitude (h) in meters, pitch angle (δ) in radians, roll angle (ρ) in radians, frontal speed (v_f), lateral (v_l) in meters per second and the inputs pitch thrust (u_δ), roll thrust (u_ρ) and altitude thrust (u_h). Given this, the states of lateral displacement (d_l) and frontal displacement (d_f) were added, which are the states controlled by the LQR. The Equation (8) shows the state space model used.

$$\begin{aligned}
\begin{bmatrix} \rho_k \\ \delta_k \\ v_{f_k} \\ v_{l_k} \\ h_k \\ d_{f_k} \\ d_{l_k} \end{bmatrix} &= \begin{bmatrix} 0.869 & 0 & 0 & 0 & 0 & 0 & 0 \\ 0 & 0.882 & 0 & 0 & 0 & 0 & 0 \\ 0 & -0.72 & 0.975 & 0 & 0 & 0 & 0 \\ 0.6 & 0 & 0 & 0.966 & 0 & 0 & 0 \\ 0 & 0 & 0 & 0 & 1 & 0 & 0 \\ 0 & T_s & 0 & 0 & 0 & 1 & 0 \\ 0 & 0 & T_s & 0 & 0 & 0 & 1 \end{bmatrix} \begin{bmatrix} \rho_{k-1} \\ \delta_{k-1} \\ v_{f_{k-1}} \\ v_{l_{k-1}} \\ h_{k-1} \\ d_{f_{k-1}} \\ d_{l_{k-1}} \end{bmatrix} \\
&+ \begin{bmatrix} 0.06 & 0 & 0 \\ 0 & -0.05 & 0 \\ 0 & 0 & 0 \\ 0 & 0 & 0 \\ 0 & 0 & 0.03 \\ 0 & 0 & 0 \\ 0 & 0 & 0 \end{bmatrix} \begin{bmatrix} u_\rho(k-d) \\ u_\delta(k-d) \\ u_h(k-d) \end{bmatrix} \\
&+ \begin{bmatrix} 0.55 & 0 & 0 & 0 & 0 \\ 0 & 0.64 & 0 & 0 & 0 \\ 0 & 0 & 0.197 & 0 & 0 \\ 0 & 0 & 0 & 0.216 & 0 \\ 0 & 0 & 0 & 0 & 0.43 \\ 0 & 0 & 0 & 0 & 0 \\ 0 & 0 & 0 & 0 & 0 \end{bmatrix} \begin{bmatrix} e_\rho(k-1) \\ e_\delta(k-1) \\ e_{vf}(k-1) \\ e_{vl}(k-1) \\ e_h(k-1) \end{bmatrix}
\end{aligned} \tag{8}$$

where T_s is the sampling time of the discrete model. This work considers positions as a result of the numerical integration of velocities. Therefore, any disturbance that affects the displacement state directly results from the disturbance in the displacement rate (velocity).

It is worth noting that the model is not a complete description of the UAV dynamics. However, this formulation accurately describes the influence of high-level control signals on the vehicle maneuver within the operating regime of the simulated experiment, where the linear system can be approximated to the dynamics of the quadcopter, as presented in the work of Santana et al. (2016).

The model in question establishes that the noise from disturbances that affect the system has a Gaussian distribution, and the variance of these noises is present in the Equation (9) with Var being the operator that extracts the variance from the noise.

$$Var(\mathbf{e}) = \begin{bmatrix} 0.00035 \\ 0.00031 \\ 0.00157 \\ 0.00199 \\ 0.0002 \end{bmatrix} \tag{9}$$

Therefore, the simulated experiment of the closed-loop system of the quadcopter's autopilot must be tuned according to its internal dynamics and considering the dynamics of the disturbances that affect the system. In this way, the simulated experiment of the closed-loop system of the quadcopter's autopilot controls the dynamics of the drone affected by the dynamics of disturbances.

2.3 ELECTRE III

The ELECTRE method was created in 1966 by Bernard Roy as part of the MCDM method family of the European School (Roy, 1966). The main characteristic and advantage of methods based on ELECTRE is that they avoid compensations between criteria and any normalization process that distorts the original data. Therefore, the control design based on ELECTRE III does not tolerate a compensation effect (for example, poor performance of control cannot be compensated by a good system robustness); therefore, the main foundation of the method is the use of so-called "outperforming relationships" to be able to establish a degree of dominance between the alternatives.

The MCDM of the ELECTRE family is based on two matrices: the agreement matrix and the disagreement matrix. The first evaluates the degree of agreement between the alternatives using the weight of the criteria as a basis; in short, the agreement tests the statement that a significant subset of criteria agree that alternative a is as good as b. The disagreement matrix evaluates the alternatives themselves (without the aid of the weights of each criterion), calculating the degree of disagreement of the alternatives, in short, those alternatives that do not agree and how much they disagree.

In the ELECTRE III method specifically, there are three matrices, the global agreement matrix, $\mathbf{CG}$, calculated based on the partial agreement matrices for each criterion, $\mathbf{C_j}$, and the partial disagreement matrices, $\mathbf{D_j}$, for each criterion. The method for establishing the partial agreement matrix is described below:

$$\mathbf{C_j}(a,b) = \begin{cases} 1\, if\ g_j(a) + q_j \geq g_j(b) \\ 0\, if\ g_j(a) + p_j \leq g_j(b) \\ otherwise,\ \frac{g_j(a) + p_j - g_j(b)}{p_j - q_j} \end{cases} \tag{10}$$

where j is the criterion being evaluated, g is the value of that criterion, and p_j and q_j are the lower veto and median veto for each criterion. Note that the partial agreement matrices have the number of columns and rows equal to

the number of alternatives in the model. With the partial agreement matrices in hand, the global agreement matrix is calculated:

$$\mathbf{CG}(a,b) = \sum\nolimits_j w_j c_j(a,b) \tag{11}$$

where w_j is the weight of each criterion used by ELECTRE III. After that, the partial disagreement matrices are calculated and expressed by the following Equation:

$$\mathbf{D_j}(a,b) = \begin{cases} 1\, if\ g_j(a) + p_j \geq g_j(b) \\ 0\, if\ g_j(a) + v_j \leq g_j(b) \\ otherwise,\ \frac{g_j(b) - p_j - g_j(a)}{v_j - p_j} \end{cases} \tag{12}$$

Since v_j is the superior veto, therefore, $q_j \leq p_j \leq v_j$. These vetoes are established in agreement with the designer to establish the degree of agreement and disagreement between the alternatives. In possession of the global agreement matrix and the partial disagreement matrices, the credibility matrix $\mathbf{\Lambda}$ is calculated, where if $\mathbf{CG}(a,b)$ is greater than $\mathbf{D_j}(a,b)$ in all criteria the credibility, $\mathbf{\Lambda}(a,b)$, is equal to 1, however, if this condition is not satisfied the calculation is made following the Equation:

$$\mathbf{\Lambda}(a,b) = \mathbf{CG}(a,b) \prod_{j \in F} \frac{1 - \mathbf{D_j}(a,b)}{1 - \mathbf{CG}(a,b)} \tag{13}$$

where F is the group of alternatives in which $\mathbf{D_j}(a,b)$ is greater than $\mathbf{CG}(a,b)$. The dominance matrix is formed with the help of the credibility matrix of the alternatives. Thus, the ELECTRE method results in the outperform rating aSb, where S means that, according to the MCDM settings, there are good reasons to consider that "alternative a is at least as good as "b" or "a" is not worse than b." Each pair of alternatives is tested to verify whether the statement S is valid or not, giving rise to one of the following situations:

- Situation 1: aSb and not bSa: "a" is preferable to "b" and "b" is not preferable to "a");
- Situation 2: not aSb and bSa: "a" is not preferable to "b" and "b" is preferable to "a";
- Situation 3: aSb and bSa: corresponds to a situation of indifference;
- Situation 4: not aSb and not bSa: corresponds to an incompatibility situation.

In this work, the criteria used in the application of ELECTRE III were the Squared Integral Error Index (ISE) and Quadratic Control Effort (ISU), both of which evaluate the performance of the control system and the gain margin and phase margin that evaluate the robustness of the project. Performance indices are calculated as follows:

$$ISE = \frac{1}{N} \sum_{k=0}^{N} \left(y(k) - r(k)\right)^2 \tag{14}$$

$$ISU = \frac{1}{N} \sum_{k=0}^{N} u(k)^2 \tag{15}$$

where $y(k)$ is the system output, $r(k)$ is the desired output and N is number of experiment samples. The ISE expresses how much the actual output deviated from the desired output, and the ISU expresses how much energy was spent to control that system; therefore, the higher these indexes, the worse the control performance. For the proposed problem, the ISE criterion is the sum of the ISE indices of the desired outputs (frontal position, lateral position, and height), and the ISU criterion is the sum of the ISU indices referring to each system input.

The robustness criteria of the optimal control algorithm are the gain margin, GM_{db}, and the phase margin, PM^o, of the closed loop system. The gain margin establishes how much the loop gain can be increased until the system becomes unstable. The phase margin establishes how much delay the control loop can handle before it becomes unstable. Therefore, the higher these indices are, the more robust the system is in terms of parametric variation and disturbances. In this work, the system functions S and T are used to calculate such indices, where T is the sensitivity function of the MIMO system controlled in a closed loop in relation output of the system and S is the complementary sensitivity function. Given this, the gain margin and phase margin are calculated as follows:

$$T + S = 1 \tag{16}$$

$$m_t = \underbrace{\max}_{\omega} \left| T(e^{-j\omega T_s}) \right| \tag{17}$$

$$m_s = \underbrace{\max}_{\omega} \left| S(e^{-j\omega T_s}) \right| \tag{18}$$

$$GM_{Db} = 20\log_{10} \left\{ \min \left[\left(\frac{m_s}{m_s - 1} \right), \left(1 + \frac{1}{m_t} \right) \right] \right\}, \tag{19}$$

$$PM^o = \left(\frac{180^o}{\pi} \right) \min \left[2sen^{-1} \left(\frac{1}{2m_s} \right), 2sen^{-1} \left(\frac{1}{2m_t} \right) \right] \tag{20}$$

where e is Euler's constant, ω is the frequency in radians and j is the imaginary unit.

2.4 Experiment Setup

In this work, the proposed task for the drone is hovering. In this task, the drone receives a specific coordinate, which is the desired location of the vehicle. This experiment is a step signal in the coordinates of frontal displacement, lateral displacement, and altitude. When arriving at the desired point, it is essential to stay in that place (or close to it) for a long time and be exposed to the most diverse disturbances caused by winds. This type of mission can occur when a catastrophe, such as a natural disaster, occurs and the place's infrastructure is compromised. In this way, UAVs equipped with antennas offer network signals to the affected area, enabling communication in the region (Erdelj et al., 2017) and assisting in the process of rescuing survivors.

The experiment was simulated in a Python environment where the hover task was performed for 500 seconds. In this

experiment, the quadcopter was exposed to disturbances such as colored noises in the stochastic model and initial states are null.

In this article, it is proposed that ELECTRE III be used to assist the designer in tuning the control that best suits the needs of each mission. For this to occur, it is necessary to establish the alternatives analyzed by MCDM. However, the variety of LQR configurations is infinite, making it necessary to reduce the sample set. To select this set, the Bryce (Deng et al., 2017) method was applied to choose the average weights of $\mathbf{Q}_a$ and $\mathbf{R}_a$ and the multi-criteria decision model alternatives are the values around the average weights. According to this rule, $\mathbf{Q}_a$ and $\mathbf{R}_a$ are diagonal matrices whose elements are expressed as the inverse squares of the maximum acceptable values of the state variable and the input control variable, respectively. The diagonal elements of the matrices $\mathbf{Q}_a$ and $\mathbf{R}_a$, therefore, can be written as:

$$\mathbf{Q}_{a_{ii}} = \frac{1}{(maximum\ acceptable\ value\ of\ x_i^2)}) \tag{21}$$

$$\mathbf{R}_{a_{ii}} = \frac{1}{(maximum\ acceptable\ value\ of\ u_i^2)} \tag{22}$$

where i are diagonal elements of the matrices. Applying the Bryce method to the weighting matrices in the extended system and depending on the conditions under which the Sodré (2024) model was estimated, we have the following values:

$$\mathbf{Q}_a = diagonal(1\ 1\ 1\ 0.1\ 0.1\ 0.1\ 0.1\ 0.1\ 0.1\ 0.1) \tag{23}$$

$$\mathbf{R}_a = diagonal(5\ 5\ 5) \tag{24}$$

With the weighting matrices suggested by the Bryce method, alternatives were raised in the values that are weighting the variables of interest, $\mathbf{Q}_i$, which are height, lateral position and frontal position. This choice is justified as there is no need to weigh the inputs, as in the proposed mission there is no priority effort over the inputs, and in states where there is no interest, modifications would not result in significant changes.

Given this, control project alternatives were created whose weights were based on the states of interest. These alternatives take on values between 0.5 and 1.5 with 0.1 spacing to weigh the positional states of the drone, creating 286 alternatives that ELECTRE III establishes preference relationships. Note that among these alternatives, a set of weights arises from the Bryce method, thus allowing a comparison between the Bryce method and the best-ranked alternatives of the proposed method.

Another important step in applying the ELECTRE III method is establishing veto values. The average distance between the criteria was calculated, and the vetoes were calculated based on these values, as shown in the Equation (25)

$$M_j = \frac{\sum_{a=1}^{N_a} \sum_{b=a+1}^{N_a} |g_j(a) - g_j(b)|}{N_d} \tag{25}$$

where M is the average of the distances between the alternatives of the criterion j, N_d is the number of distances, and N_a is the number of alternatives. In possession of the averages, ELECTRE III vetoes the following values:

$$\mathbf{q} = [0.9M_{ISU}\ 0.9M_{ISE}\ 0.9M_{GM_{Db}}\ 0.9M_{PM^o}] \tag{26}$$

$$\mathbf{p} = [M_{ISU}\ M_{ISE}\ M_{GM_{Db}}\ M_{PM^o}] \tag{27}$$

$$\mathbf{v} = [1.1M_{ISU}\ 1.1M_{ISE}\ 1.1M_{GM_{Db}}\ 1.1M_{PM^o}] \tag{28}$$

In this way, the vetoes are calculated according to the performance of each tuning, considering the indexes of all LQR configurations to rank the alternatives.

Finally, it is necessary to define the gain of each criterion as necessary for the mission. Therefore, the system's lower energy consumption and greater robustness were valued at the expense of reference tracking in the hovering task. This consideration was made due to the need for the four-engine engine to remain in a fixed position for a long time, which is exposed to disturbances from the most different frequencies, requiring less control effort, increasing flight time, and avoiding rapid battery discharge. For this mission, the weight vector has the following gains:

$$\mathbf{w} = [0.4\ 0.1\ 0.25\ 0.25] \tag{29}$$

3. EXPERIMENT

In the experiment of the method proposed by this work, control strategies are simulated, and based on these simulations, the values of each criterion are extracted to support the ranking of control tunings by ELECTRE III. The best-ranked control configuration was the one in which the matrix $\mathbf{Q}$ had the following weights in the states of interest: $\mathbf{Q}_i = [0.5, 0.8, 1.2]$. This configuration is represented by the alternative a_{35} in the graph in Figure 1.

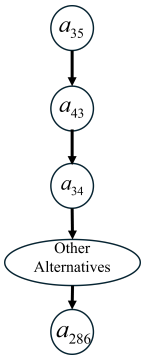

Figure 1. Experiment Graph

This graph represents the dominance relationships of alternatives, where the arrow's base is the dominant and the arrow's tip finds the dominated alternative. Therefore, alternative 35 dominates (outperforms) the other alternatives, thus being the alternative best suited to the weights of the alternatives. Criteria established for ELECTRE III. The LQR tuning experiment proposed by the ELECTRE III Multicriteria Decision Model and the experiment using the weighting matrices of the Bryce Method can be seen in Figures 2, 3 and 4.

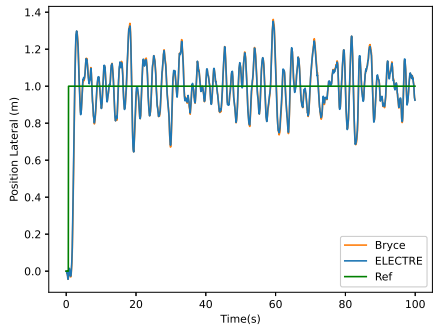

(a) Lateral Position

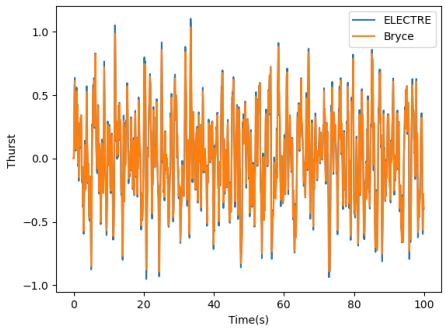

(b) Roll Thrust

Figure 2. Lateral Position Mesh

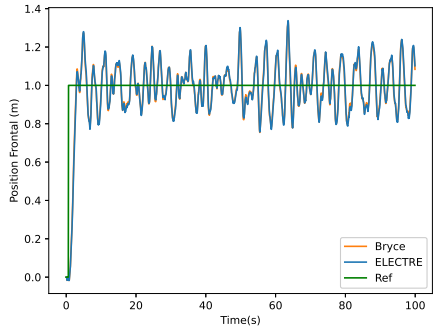

(a) Front Position

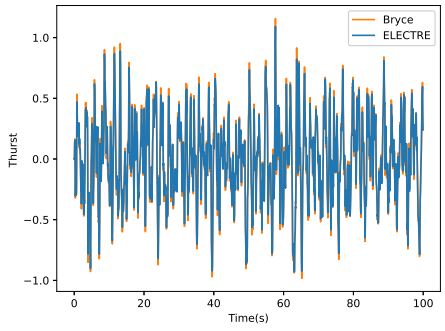

(b) Pitch Thrust

Figure 3. Front Position Mesh

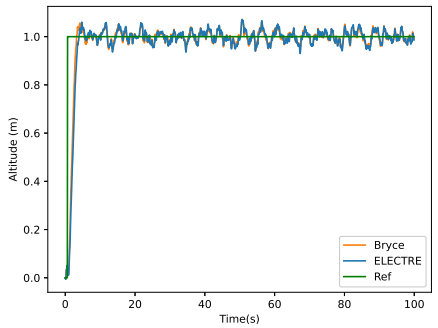

(a) Altitude

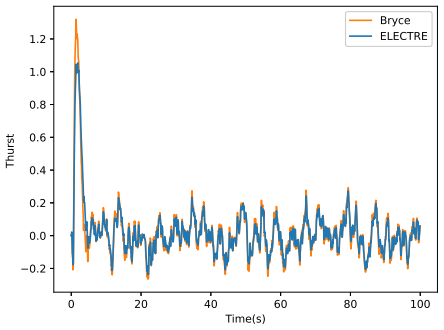

(b) Altitude Thrust

Figure 4. Altitude Mesh

Note that in terms of output performance, the best-ranked alternative in the ELECTRE III model is similar to the Bryce method. However, when analyzing the control effort, note that ELECTRE opted for a weight configuration different from that suggested by the Bryce method. Energy expenditure, in general, was lower, especially concerning the mesh regarding the height of the four-engine; this is due to the drone's altitude control requiring more effort than the rest of the meshes. Therefore, the MCDM allocated the energy resource to frontal and lateral displacement meshes at the expense of altitude.

In addition to control performance, ELECTRE III considered system robustness criteria in its classification process. Table 1 shows the most essential alternatives and their respective indexes.

Options	Order	Q_i	ISU	ISE	GM	PM^o
a_{35}	1^o	[0.5,0.8,1.2]	0.268	0.033	6.03	32.75
a_{43}	2^o	[0.5,0.9,1.3]	0.27	0.032	6.025	32.65
a_{34}	3^o	[0.5,0.8,1.1]	0.263	0.034	6.027	32.70
Bryce	51^o	[1.0,1.0,1.0]	0.272	0.032	6.020	32.61
a_{286}	286^o	[1.5,1.5,1.5]	0.324	0.029	6.020	32.47

Table 1. Alternative Indexes

The Table 1 demonstrates the relevant choice of ELECTRE III. The best-placed alternatives have the weighting matrix **Q** with similar values. The alternative surpassed by the others (286) presents this experiment's most aggressive LQR configuration, having a better ISE index than the others. Still, this characteristic comes at the cost of exert-

ing more significant control effort and less robustness in the closed-loop system. Therefore, it did not obtain better results than other alternatives in the most valued criteria in the proposed multi-criteria decision model. Another critical point to highlight is how ELECTRE III avoided the criteria compensation process, as the alternative a_{34} is in third position in the ranking, even though it costs less energy than the best-ranked alternatives. However, this characteristic did not polarize ELECTRE in its analysis, which opted for configurations capable of better reference tracking than absolute energy savings.

4. CONCLUSION

This work used ELECTRE III to assist choose the values of the LQR weighting matrices applied to the autopilot of a quadcopter model UAV. ELECTRE III was tasked with choosing the configuration that best suits the drone's hovering maneuver. The result of this experiment was the ranking of different control settings that meet the project criteria, and the best-ranked alternative presented the most appropriate behavior for the mission objectives. Furthermore, this proposed method can be used interactively, reducing the value of the spacing between control tunings and making it possible to find more precise tunings with the project objectives. In future work, we intend to increase the number of criteria and establish experiments that consider other aspects of the design outside the control and automation area. Another approach is to use the proposed method in other missions that UAVs usually perform, such as landing, takeoff, cargo movement, trajectory tracking, and others.

REFERENCES

David W. Casbeer, Derek B. Kingston, R.W.B. and McLain, T.W. (2006). Cooperative forest fire surveillance using a team of small unmanned air vehicles. *International Journal of Systems Science*, 37(6), 351–360. doi:10.1080/00207720500438480. URL `https://doi.org/10.1080/00207720500438480`.

Deng, X., Sun, X., Liu, R., and Wei, W. (2017). Optimal analysis of the weighted matrices in lqr based on the differential evolution algorithm. In *2017 29th Chinese Control And Decision Conference (CCDC)*, 832–836. IEEE.

Elkhatem, A.S. and Engin, S.N. (2022). Robust lqr and lqr-pi control strategies based on adaptive weighting matrix selection for a uav position and attitude tracking control. *Alexandria Engineering Journal*, 61(8), 6275–6292.

Erdelj, M., Natalizio, E., Chowdhury, K.R., and Akyildiz, I.F. (2017). Help from the sky: Leveraging uavs for disaster management. *IEEE Pervasive Computing*, 16(1), 24–32.

Joelianto, E., Christian, D., and Samsi, A. (2020). Swarm control of an unmanned quadrotor model with lqr weighting matrix optimization using genetic algorithm. *Journal of Mechatronics, Electrical Power, and Vehicular Technology*, 11(1), 1–10.

Khatoon, S., Shahid, M., Ibraheem, and Chaudhary, H. (2014). Dynamic modeling and stabilization of quadrotor using pid controller. In *2014 International Conference on Advances in Computing, Communications and Informatics (ICACCI)*, 746–750. doi:10.1109/ICACCI.2014.6968383.

Kumar, V. and Jerome, J. (2016). Algebraic riccati equation based q and r matrices selection algorithm for optimal lqr applied to tracking control of 3rd order magnetic levitation system. *Archives of Electrical Engineering*, 65(1), 151–168.

López, J., Dormido, R., Dormido, S., Gómez, J., et al. (2015). A robust controller for an uav flight control system. *The Scientific World Journal*, 2015.

Ogata, K. (1996). *Sistemas de control en tiempo discreto*. Pearson educación.

Reyes-Valeria, E., Enriquez-Caldera, R., Camacho-Lara, S., and Guichard, J. (2013). Lqr control for a quadrotor using unit quaternions: Modeling and simulation. In *CONIELECOMP 2013, 23rd International Conference on Electronics, Communications and Computing*, 172–178. doi:10.1109/CONIELECOMP.2013.6525781.

Roy, B. (1966). Méthodologie multicritère d'aide à la décision. *Revue Française d'Automatique, Informatique et Recherche Opérationnelle*, 10(8), 77–186.

Santana, L.V., Brandão, A.S., and Sarcinelli-Filho, M. (2016). Navigation and cooperative control using the ar. drone quadrotor. *Journal of Intelligent & Robotic Systems*, 84, 327–350.

Silveira, A., Silva, A., Coelho, A., Real, J., and Silva, O. (2020). Design and real-time implementation of a wireless autopilot using multivariable predictive generalized minimum variance control in the state-space. *Aerospace Science and Technology*, 105, 106053.

Sodré, L. (2024). *Controle Linear Quadrático Gaussiano de um Quadricóptero Baseado em um Filtro de Kalman Estendido com Variável Instrumental*. Master's thesis.

Srikanth, M. and Yadaiah, N. (2020). Optimal parameter tuning of modified active disturbance rejection control for unstable time-delay systems using an ahp combined multi-objective quasi-oppositional jaya algorithm. *Applied Soft Computing*, 86, 105881.

Srikanth, M. and Yadaiah, N. (2021). Analytical tuning rules for reduced-order active disturbance rejection control with fopdt models through multi-objective optimization and multi-criteria decision-making. *ISA transactions*, 114, 370–398.

Tahir, Z., Jamil, M., Liaqat, S.A., Mubarak, L., Tahir, W., and Gilani, S.O. (2016). Design and development of optimal control system for quad copter uav. *Indian Journal of Science and Technology*, 9(25), 10–17485.

Wang, Z., Wen, M., Dang, S., Yu, L., and Wang, Y. (2021). Trajectory design and resource allocation for uav energy minimization in a rotary-wing uav-enabled wpcn. *Alexandria Engineering Journal*, 60(1), 1787–1796. doi:https://doi.org/10.1016/j.aej.2020.11.027. URL `https://www.sciencedirect.com/science/article/pii/S1110016820306098`.

Wang, Z., Han, Y., Geng, Z., Zhu, Q., Xu, Y., and He, Y. (2017). Pid control loop performance assessment and diagnosis based on dea-related mcda. In *2017 6th International Symposium on Advanced Control of Industrial Processes (AdCONIP)*, 535–540. IEEE.

Xiong, J.J. and Zhang, G. (2016). Sliding mode control for a quadrotor uav with parameter uncertainties. In *2016 2nd International Conference on Control, automation and robotics (ICCAR)*, 207–212. IEEE.